Electronic Supplementary Information for:

VUV-UV-vis photoluminescence, X-ray radioluminescence and energy transfer dynamics of Ce^{3+} and Eu^{2+} in $Sr_2MgSi_2O_7$

Donghao Wen [a], Quanfeng Li [a], Yiyi Ou [a], Yunlin Yang [a], Zeming Qi [b], Pieter Dorenbos [c], Hongbin Liang *[a]

[a] *MOE Key Laboratory of Bioinorganic and Synthetic Chemistry, KLGHEI of Environment and Energy Chemistry, School of Chemistry, Sun Yat-sen University, Guangzhou 510006, China*

[b] *National Synchrotron Radiation Laboratory, University of Science and Technology of China, Hefei 230029, China*

[c] *Faculty of Applied Sciences, Delft University of Technology, 2629 JB, Delft, The Netherlands*

* E-mail: cesbin@sysu.edu.cn (Hongbin Liang).

Contents

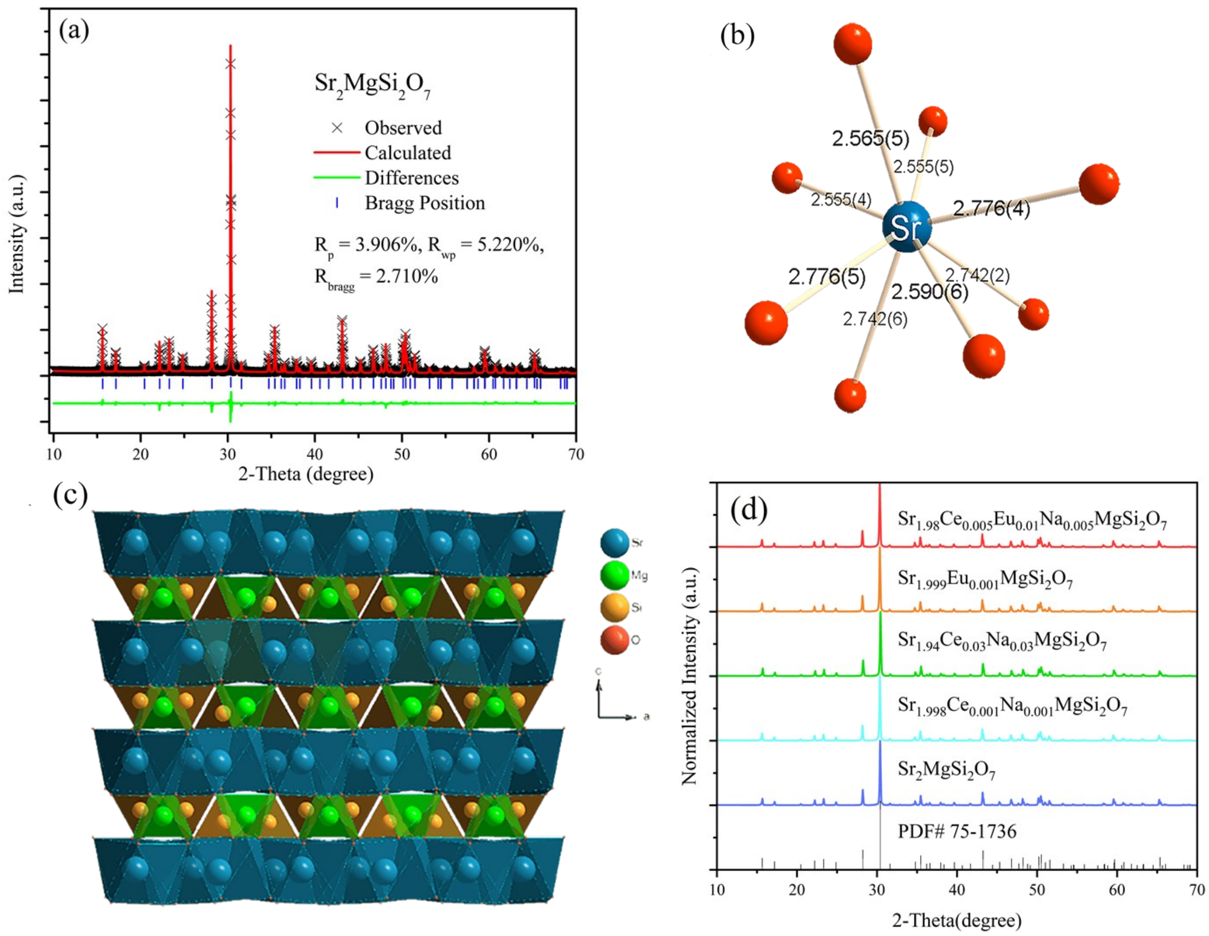

Fig. S1 (a) The Rietveld refinement of laboratory high quality XRD data of the $Sr_2MgSi_2O_7$ sample at RT. (b) The coordination environments of a Sr^{2+} site and the Sr^{2+}-O^{2-} bond lengths (Å). (c) The crystal structure of $Sr_2MgSi_2O_7$. (d) The XRD patterns of $Sr_{2-2x}Ce_xNa_xMgSi_2O_7$ (x = 0.001, 0.03), $Sr_{2-x}Eu_xMgSi_2O_7$ (x = 0.001) and $Sr_{1.99-x}Ce_{0.005}Eu_xNa_{0.005}MgSi_2O_7$ (x = 0.01) samples at RT.

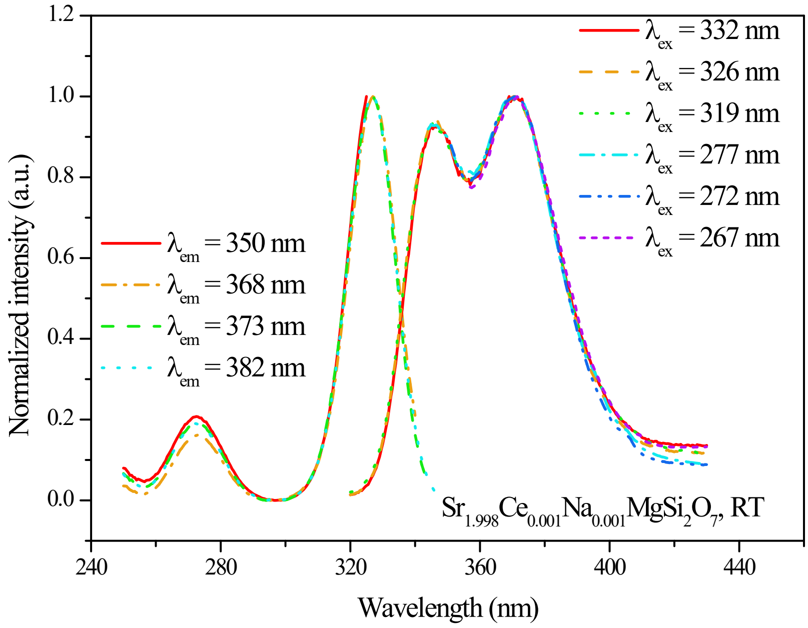

Fig. S2 The height normalized excitation (λ_{em} = 350, 368, 373, 382 nm) and emission (λ_{ex} = 267, 272, 277, 319, 326, 332 nm) spectra of the sample $Sr_{1.998}Ce_{0.001}Na_{0.001}MgSi_2O_7$ at RT.

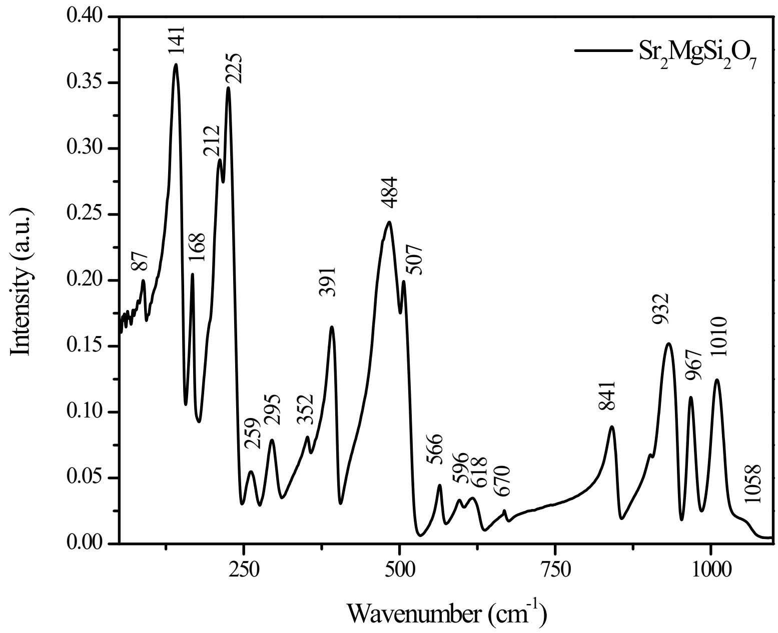

Fig. S3 The synchrotron radiation far infrared reflectance spectrum of $Sr_2MgSi_2O_7$ at RT.

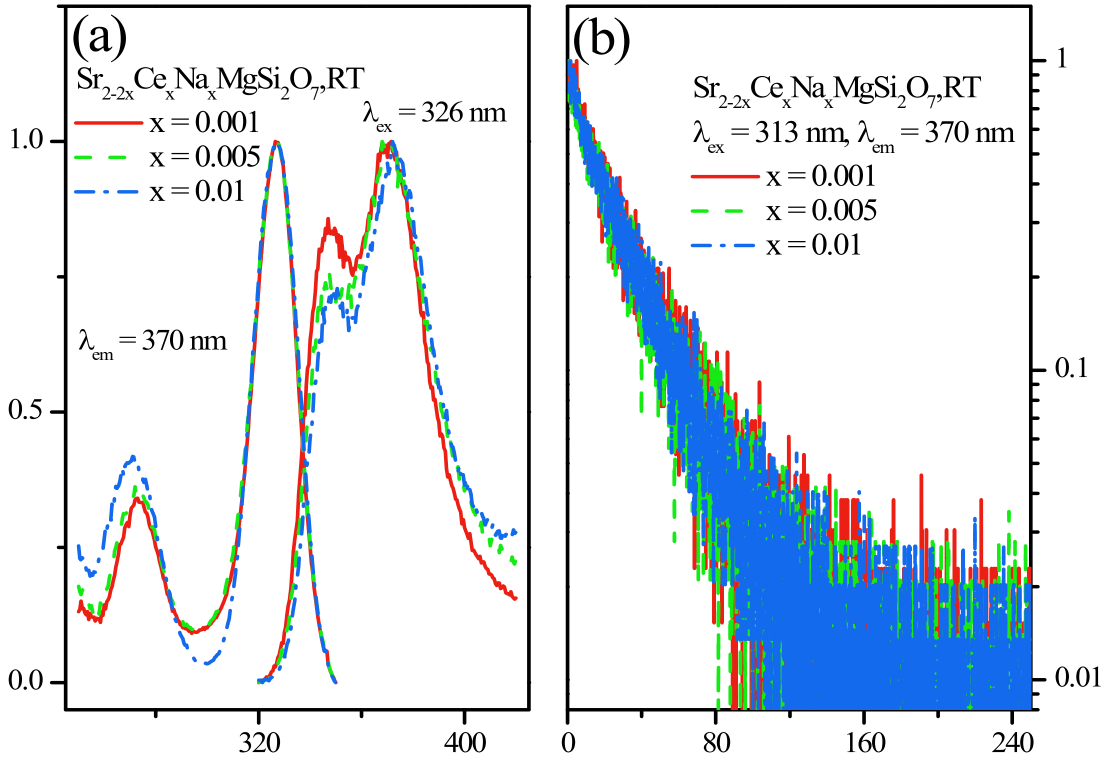

Fig. S4 (a) The height normalized excitation (λ_{em} = 370 nm) and emission (λ_{ex} = 273 nm) spectra and (b) luminescence decay curves (λ_{ex} = 313 nm, λ_{em} = 370 nm) of the samples $Sr_{2-2x}Ce_xNa_xMgSi_2O_7$ (x = 0.001, 0.005, 0.03) at RT.

The Ce^{3+} doping concentration dependent luminescence is studied. The height normalized excitation (λ_{em} = 370 nm) and emission (λ_{ex} = 273 nm) spectra of the samples $Sr_{2-2x}Ce_xNa_xMgSi_2O_7$ (x = 0.001, 0.005, 0.03) at RT are shown in Fig. S4(a) for comparison. The change of doping concentration of Ce^{3+} almost makes no difference to the excitation peak at ~326 nm, implying that the lowest 5d state energy is quite stable for different doping concentrations. The emission peak position of 5d-$^2F_{5/2}$ remains unchanged at ~345 nm but the emission intensity ratio of 5d-$^2F_{7/2}$ to 5d-$^2F_{5/2}$ increases with the increasing concentrations due to the reabsorption.

The luminescence decay curves of the samples $Sr_{2-2x}Ce_xNa_xMgSi_2O_7$ (x = 0.001, 0.005, 0.03) at RT are shown in Fig. S4(b). All decay curves overlap with each other and follow exponential characteristic, and the lifetime is estimated to be

27.2 ns, implying that concentration quenching does not occur in the studied concentration range. The lifetime at RT in Fig. S4(b) is consistent with that at 78K in the inset of Fig. 1, implying that temperature quenching does not occur below RT.

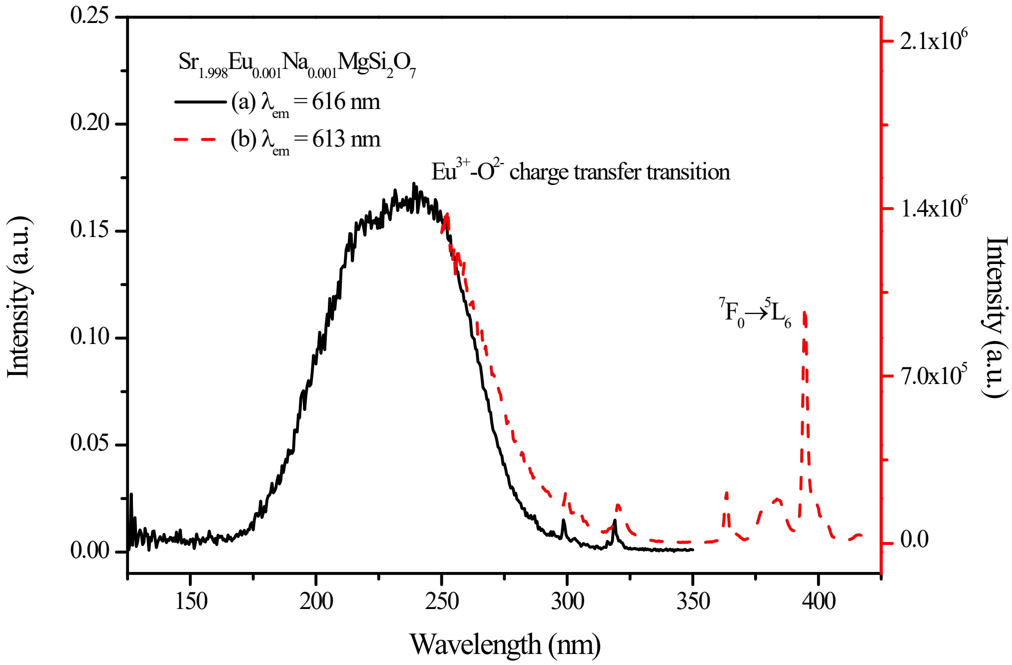

Fig. S5 The VUV-UV excitation (a, λ_{em} = 616 nm, 10 K) and UV-vis excitation (b, λ_{em} = 613 nm, RT) spectra of $Sr_{1.998}Eu_{0.001}Na_{0.001}MgSi_2O_7$.

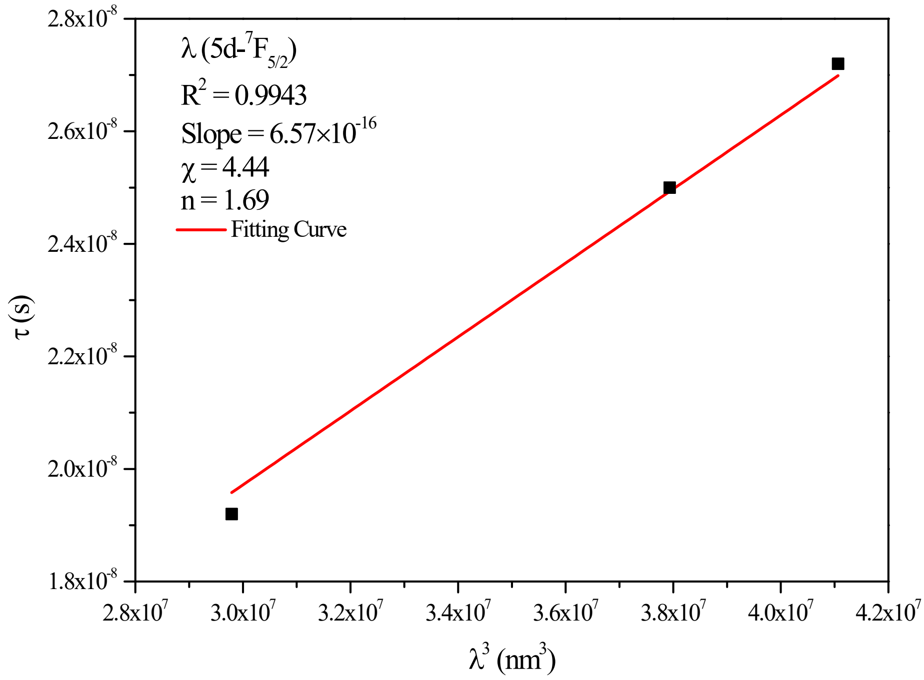

Fig. S6 The λ^3-τ relationship of Ce^{3+} in $Sr_2MgSi_2O_7$, $Ba_2MgSi_2O_7$ and $BaMg_2Si_2O_7$.

Table S1 Thermal quenching activation energy (E_a), reciprocal of intrinsic lifetime (Γ_v), thermal-quenching rate at T = ∞ (Γ_0) and coefficients of determination of fitting procedure (R^2) via equations (6) and (7).

Eu^{2+}	E_a (eV)	Γ_v (s^{-1})	Γ_0 (s^{-1})	R^2
Integrated intensity	0.226	1.73×10^6	1.84×10^{10}	0.989
Lifetime	0.252	1.76×10^6	4.83×10^{10}	0.999

Table S2 The S value, energy transfer microparameters (C_{DA}), energy migration microparameters (C_{DD}) and coefficients of determination of fitting procedure (R^2) via Inokuti-Hirayama (IH), Yokota-Tanimoto (YT) and Burshteĭn model.

Model	S	C_{DA} ($m^6 \cdot s^{-1}$)	C_{DD} ($m^6 \cdot s^{-1}$)	R^2
IH	6	2.89×10^{-45}	-	0.998
IH	8	1.82×10^{-62}	-	0.997
IH	10	7.98×10^{-80}	-	0.996
YT	6	2.35×10^{-46}	1.03×10^{-45}	0.992
Burshteĭn	6	1.16×10^{-46}	9.02×10^{-45}	0.997